Research Article

Investigation of Magnetic Nanoparticle Motion under a Gradient Magnetic Field by an Electromagnet

Weizhong Wei [1] **and Zhen Wang** [2,3]

[1] *Wuhan Children's Hospital (Wuhan Maternal and Child Healthcare Hospital), Tongji Medical College,*
 Huazhong University of Science and Technology, Wuhan 430074, China
[2] *Wuhan National High Magnetic Field Center, Huazhong University of Science and Technology, Wuhan 430074, China*
[3] *State Key Laboratory of Advanced Electromagnetic Engineering and Technology, Huazhong University of Science and Technology,*
 Wuhan 430074, China

Correspondence should be addressed to Zhen Wang; evawong@hust.edu.cn

Finite element numerical simulations were carried out in 2D geometry to calculate the magnetic force on magnetic nanoparticles under a specially fabricated electromagnet. The particle motion was modeled by a system of ordinary differential equations. The snapshots of trajectories of 4000 MNPs with and without magnetic field were analyzed and qualitatively found to be in agreement with camera visualizations of MNP movement in a container. The results of the analysis could be helpful for the design of electromagnetic field and motion analysis of magnetic particles for the delivery of magnetic materials in biomedical applications.

1. Introduction

Magnetic nanoparticle (MNP) is a material of interest for biological and biomedical applications [1]. The principle of MNP transport is based on the magnetic polarization and magnetophoretic mobility when an external magnetic field gradient is applied [2]. The behavior of MNPs under a magnetic field, relating to the magnetic properties of carriers and the performance of magnet systems, depends on the interplay of the magnetic force, Stokes drag, and diffusive motions acting on the particles [3, 4]. To effectively manipulate the MNPs, it is necessary to ensure the generated magnetic force is strong enough, and its efficiency can be estimated and predicted by analysis of MNP motion before the fabrication of a system.

Typically, gradient magnetic fields are used for manipulating these MNPs, which can be usually generated by either permanent magnets [5, 6] or electromagnets [7, 8]. Note that a characteristic feature of these magnetic manipulation systems is that MNPs will be attracted towards the surface of magnets, while they are hard to be focused at a position away from magnet surface [9]. Interestingly, Pei et al. [10] proposed a novel structure of an electromagnet that is based on the magnetic field fringing effect to change the magnetic field distribution, which has been demonstrated to be an effective tool for deep magnetic capture [11]. This type of electromagnet could have a great potential for deep targeting in the body. The existing studies utilizing the special magnet have just focused on the investigation of particle motion behavior in a cylindrical space that is located in the central part of the electromagnet [10–12], while the particle distribution in a large region around the magnet has not been reported.

In this work, to further fully understand the dynamic behavior of MNPs under the special gradient magnetic field, a similar electromagnetic apparatus is designed and fabricated. On this basis, by means of numerical simulations using COMSOL and Matlab software, the magnetic force acting on the MNPs and the trajectories of MNPs in a static ferrofluid under a magnetic field are investigated in detail. Finally to corroborate the simulation results, the distribution of MNPs in a narrow rectangular container was visualized by a camera.

2. Theoretical Model and Numerical Simulation

There are mainly two forces acting on the MNP of the ferrofluid under magnetic field: (1) the magnetic force, $\overrightarrow{F_m}$, which is generated by the applied magnetic field gradient, and (2) the fluidic force, $\overrightarrow{F_s}$, which is exerted by the suspending medium on a moving MNP. Other forces, such as buoyancy, the gravitational force, and the interaction between particles, can be neglected for MNPs in the fluid [13]. The magnetic force on the particles is usually derived by the following formula [14]:

$$\overrightarrow{F_m} = \mu_0 V_m \chi \left(\overrightarrow{H_a} \cdot \nabla \right) \overrightarrow{H_a}, \tag{1}$$

where μ_0 is the magnetic permeability of free space, V_m is the volume of the particle, χ is the magnetic susceptibility, and $\overrightarrow{H_a}$ is the applied external magnetic field.

The fluidic force for a spherical particle is determined by Stokes' law:

$$\overrightarrow{F_s} = -6\pi\eta r_p \left(\overrightarrow{v_p} - \overrightarrow{u} \right), \tag{2}$$

where r_p and $\overrightarrow{v_p}$ are the hydrodynamic radius and velocity of the particle and η and $\overrightarrow{u}$ are the viscosity and velocity of the fluid, respectively. Since the magnetic susceptibility of MNPs was measured based on the total magnetic particle, the magnetic radius in (1) and the hydrodynamic radius in (2) can be considered equal, and then the volume of particle V_m in (1) can be expressed by $(4/3)\pi r_p^3$. The motion of MNP in the magnetic field and viscous fluid can be described using Newton's law:

$$m_p \frac{d\overrightarrow{v_p}}{dt} = \mu_0 V_m \chi \left(\overrightarrow{H_a} \cdot \nabla \right) \overrightarrow{H_a} - 6\pi\eta r_p \overrightarrow{v_p}. \tag{3}$$

Considering the fluid is in a static condition in the experiment, the velocity of the fluid $\overrightarrow{u}$ can be set as 0. Since MNPs acquire the terminal velocity very fast, it is considered acceptable to neglect the inertial term.

The position vectors of MNPs in the magnetic field and fluid field can be described by a cylindrical coordinate system of ordinary differential equations (ODE):

$$\frac{d\overrightarrow{r}}{dt} = v_{pr} = \frac{\overrightarrow{F_{mr}}}{6\pi\eta r_p},$$

$$\frac{d\overrightarrow{z}}{dt} = v_{pz} = \frac{\overrightarrow{F_{mz}}}{6\pi\eta r_p}, \tag{4}$$

where $(\overrightarrow{r}, \overrightarrow{z})$ is the position vector of MNP, $\overrightarrow{v_{pr}}$ and $\overrightarrow{v_{pz}}$ are the two components of MNP velocity, and $\overrightarrow{F_{mr}}$ and $\overrightarrow{F_{mz}}$ are the two components of magnetic force. The origin of the cylindrical coordinate system is strictly located at the geometric center of coils and the container. To obtain the parameters of the magnetic force, a two-dimensional

axisymmetric finite element model of the electromagnet was built and solved by COMSOL Multiphysics 3.5a using the magnetostatic module. Then the data of computed magnetic flux density and gradient was extracted from COMSOL and used for calculation of particle trajectory based on (4) using the software Matlab 7.0. Initial conditions for calculations were randomly positions for MNPs in the container with a radius of 0.02 mm and zero initial velocity. Computation of trajectories was stopped for MNPs which have arrived at the wall boundaries of the container, approximately at the distance of 5 mm from the center.

3. Experimental Configuration

An electromagnet was manufactured (Figure 1(a)) with the design method reported by Pei et al. [10]. The coils have 18 layers of $2 \times 4 \, mm^2$ copper wires, and the number of windings in each coil is 22. The magnetic pole with the coil was cylindrical with a hole in the middle. The radius of the hole is 6.5 mm, the outside radius of the pole is 30 mm, and the distance between two poles is 24 mm. The inner radius, outside radius, height, and distance of the two coils are 25 mm, 70 mm, 100 mm, and 68 mm, respectively. The dimension of the narrow container shown in Figure 1(b) is $120 * 4 * 10$ mm (length $*$ width $*$ height).

The experimental water-soluble ferrofluid was supplied by Sundia MediTech Company, Ltd., Shanghai. The MNPs are made of iron oxide grains (Fe_3O_4) coated with silicon dioxide in the ferrofluid, which have a hydrodynamic radius of 100 nm, a concentration of 40 mg/ml, and a measured magnetic susceptibility of 1.17 in the case of low field. According to the magnetization curve of the MNP (measured by SQUID-VSM), the saturation magnetization strength of these MNPs is approximately at 380 kA/m when the magnetic field strength reaches about 750 mT.

4. Results and Discussion

Figure 2 shows the magnetic field and magnetic force distribution in the positive r-axis part of the rectangular container based on a simplified 2D model in Figure 1(b). The magnetic force distribution can be used to determine where MNPs may be transported. When there is no magnetic field, the MNPs are uniformly distributed in the container region in Figure 3(a). When there is an external gradient magnetic field, the MNPs will be transported under the magnetic force. In the central region, where r is less than 10 mm, the z component of the magnetic force has a negative value in the upper part and a positive value in the lower part, concentrating the MNPs towards the middle part. Thus two blank areas appear in the central region of the container, as shown in Figure 3(b). The phenomenon basically agreed with the existing studies [10, 11]. But as time passes, we find that the two blank areas increase in Figures 3(c) and 3(d), showing that the MNPs in the central region move to the right side of the simulation region. This is because there is a positive r component of the magnetic force, as shown in Figure 2(b). Similar phenomena appear on the right hand side of the simulation region where the number of MNPs has reduced,
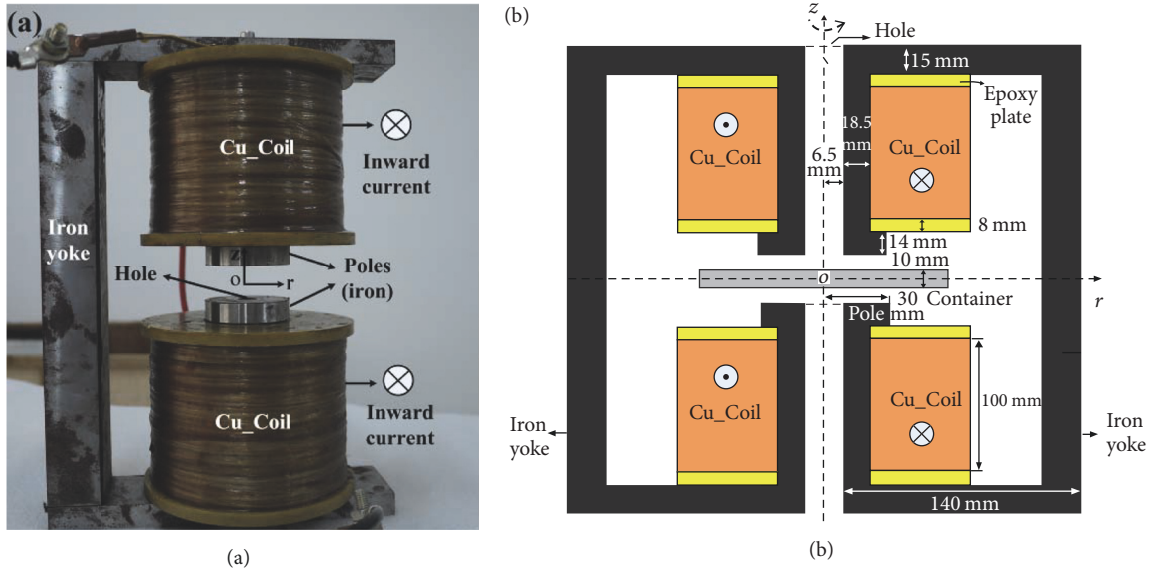
(a)

(b)

FIGURE 1: (a) Experimental electromagnet; (b) a simplified 2D axisymmetric model. The C-shaped iron yoke in (a) can be modeled as a cylindrical shape in (b) because the magnetic flux converging effect is much the same for the two shapes when the C-shaped yoke is not saturated.
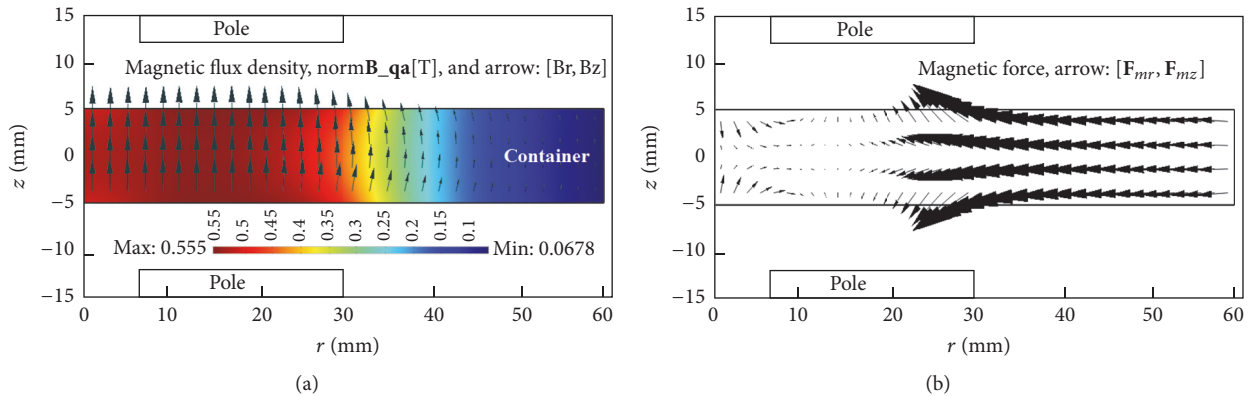

(a)

(b)

FIGURE 2: Magnetic field and magnetic force distribution in the positive half part of the rectangular container based on a simplified 2D model in Figure 1(b). (a) Magnetic flux density, norm**B_qa**, and the arrows of the two components of the field; (b) the arrows of $\mathbf{F}_{mr}$ and $\mathbf{F}_{mz}$. The current density in the coil in the simulation was set as $4e6$ A/m^2 in accordance with the current flowing in the coil ($\approx$32 A) in the experiment.

which is due to the negative r component of the magnetic force in Figure 2(b). Since the color of the magnetic fluid depends on the MNP concentration, an entire black area in the container was captured in Figure 4(a) and two small light-colored areas due to the low concentration can be seen in Figure 4(b). By comparison to the intermediate stages of the results in Figures 3 and 4, the MNPs distribution has a similar variation law with time in the simulation and experiment.

However, it should be noted that the MNPs move much faster in the simulation than that in the experiment, which can be seen from the time parameters in Figures 3 and 4. The main reasons for this phenomenon are related to the following two factors: (1) magnetic particles can be aggregated under the action of magnetic interactions between particles which has been widely mentioned in the studies relevant to magnetic manipulation of particles [14–16] and the formation of elongated aggregates will accelerate the process

of particle focusing [17, 18]. (2) Hydrodynamic interactions between particles could aid the focusing of magnetic particles [19–21]. Considering the MNP aggregation process has a little effect on the final MNP distribution, it is reasonable to validate the proposed numerical procedure according to the intermediate stages of MNP distribution by comparing the simulated results in Figure 3 and images of MNPs distribution in Figure 4.

5. Conclusion

We have proposed the numerical procedure using COMSOL and Matlab software to calculate the MNPs trajectories in a stationary magnetic liquid under a magnetic field. The simulations were qualitatively compared by camera visualizations of MNP distribution in a narrow transparent container. Different from the existing studies, we find that the MNPs
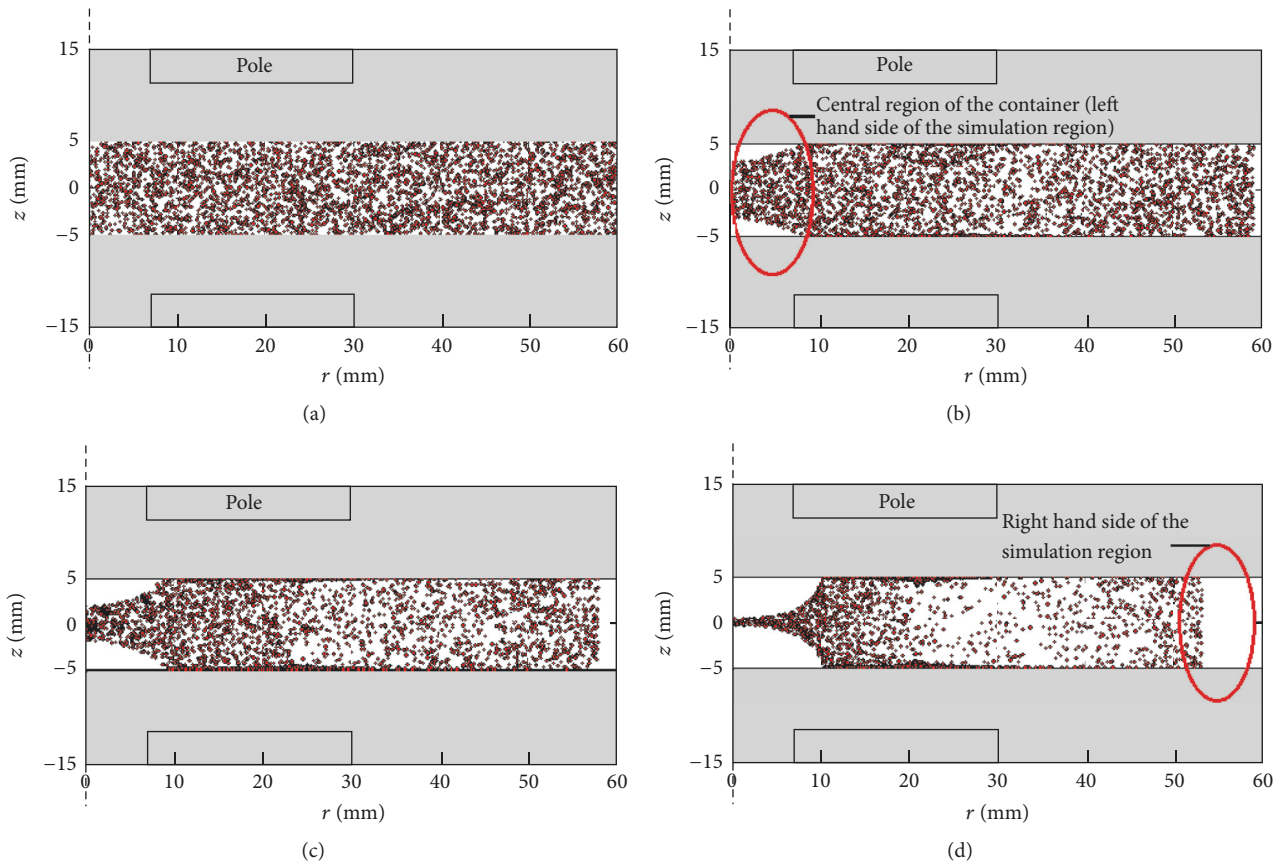
(a)

(b)

(c)

(d)

FIGURE 3: Positions of 4000 MNPs in the magnetic fluid: (a) without magnetic field, (b) with magnetic field for 800 s, (c) with magnetic field for 1600 s, and (d) with magnetic field for 4000 s. Note that only the positive half part of polar coordinate of the electromagnet in Figure 1(b) is shown in this figure.
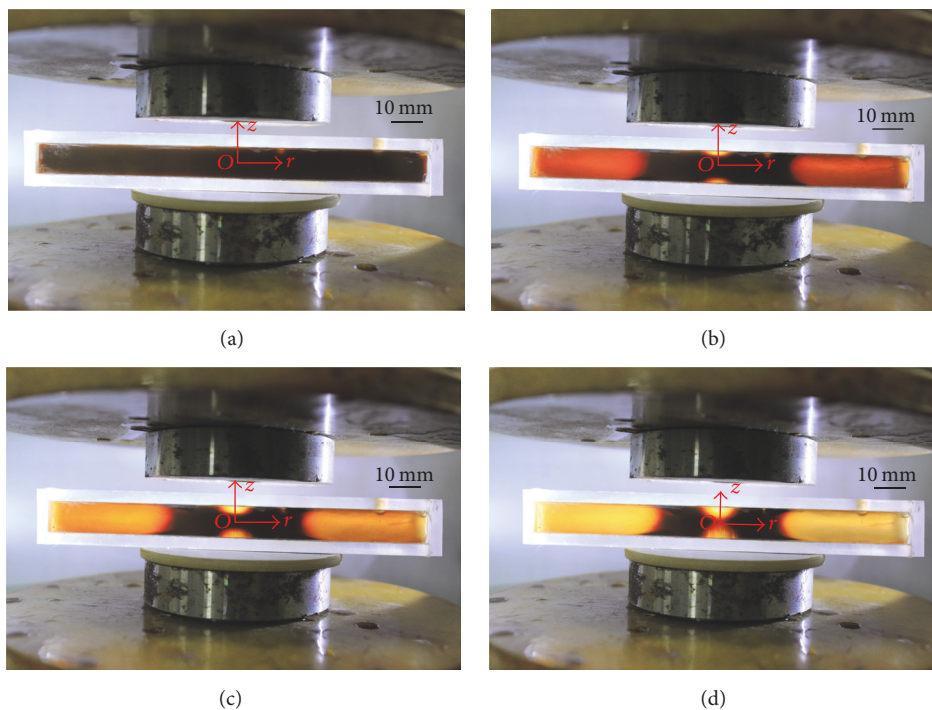

(a)

(b)

(c)

(d)

FIGURE 4: Images of MNPs distribution in a transparent plastic tube: (a) without magnetic field, (b) with magnetic field for 20 s, (c) with magnetic field for 40 s, and (d) with magnetic field for 100 s.

do not eventually accumulate in the central region of the given container, but are attracted towards the outer ring of the magnet hole. Meanwhile, it has been found that numerical procedure can approximately predict the shape and position of the MNP capture in the absence of a flow, while the simulation time required for a specific distribution is larger than that in the experiment under the same conditions. The actual MNP aggregation effect should be estimated and considered to predict exactly the MNP motion with a flow in the experiment in the future research.

Conflicts of Interest

The authors declare that they have no conflicts of interest.

References

[1] Q. A. Pankhurst, N. K. T. Thanh, S. K. Jones, and J. Dobson, "Progress in applications of magnetic nanoparticles in biomedicine," *Journal of Physics D: Applied Physics*, vol. 42, no. 22, pp. 1–13, 2009.

[2] X. Han, Y. Feng, Q. Cao, and L. Li, "Three-dimensional analysis and enhancement of continuous magnetic separation of particles in microfluidics," *Microfluidics and Nanofluidics*, vol. 18, no. 5-6, pp. 1209–1220, 2015.

[3] A. Nacev, C. Beni, O. Bruno, and B. Shapiro, "The behaviors of ferromagnetic nano-particles in and around blood vessels under applied magnetic fields," *Journal of Magnetism and Magnetic Materials*, vol. 323, no. 6, pp. 651–668, 2011.

[4] H. Y. Lee, B. K. Wu, and M. Y. Chern, "Schottky photodiode fabricated from hydrogen-peroxide-treated ZnO nanowires," *Applied Physics Express*, vol. 6, no. 5, Article ID 054103, 3 pages, 2013.

[5] V. I. Furdui and D. J. Harrison, "Immunomagnetic T cell capture from blood for PCR analysis using microfluidic systems," *Lab on a Chip*, vol. 4, no. 6, pp. 614–618, 2004.

[6] N. Pamme and A. Manz, "On-chip free-flow magnetophoresis: continuous flow separation of magnetic particles and agglomerates," *Analytical Chemistry*, vol. 76, no. 24, pp. 7250–7256, 2004.

[7] B. Gleich, N. Hellwig, H. Bridell et al., "Design and Evaluation of Magnetic Fields for Nanoparticle Drug Targeting in Cancer," *IEEE Trans. Nanotechnol*, vol. 6, no. 2, pp. 164–170, 2007.

[8] Q. Cao, X. Han, and L. Li, "An active microfluidic mixer utilizing a hybrid gradient magnetic field," *International Journal of Applied Electromagnetics and Mechanics*, vol. 47, no. 3, pp. 583–592, 2015.

[9] Q. Cao, X. Han, and L. Li. J. Magn, "Enhancement of the efficiency of magnetic targeting for drug delivery: Development and evaluation of magnet system," *Journal of Magnetism and Magnetic Materials*, vol. 323, no. 15, pp. 1919–1924, 2011.

[10] N. Pei, Z. Huang, W. Ma, J. Ge, and W. Zheng, "In vitro study of deep capture of paramagnetic particle for targeting therapeutics," *Journal of Magnetism and Magnetic Materials*, vol. 321, no. 18, pp. 2911–2915, 2009.

[11] Z. Huang, N. Pei, Y. Wang et al., "Deep magnetic capture of magnetically loaded cells for spatially targeted therapeutics," *Biomaterials*, vol. 31, no. 8, pp. 2130–2140, 2010.

[12] N. Pei, X. Cheng, Z. Huang et al., "Aggregation process of paramagnetic particles in fluid in the magnetic field," *Bioelectromagnetics*, vol. 37, no. 5, pp. 323–330, 2016.

[13] J. W. Haverkort, S. Kenjereš, and C. R. Kleijn, "Magnetic particle motion in a Poiseuille flow," *Physical Review E: Statistical, Nonlinear, and Soft Matter Physics*, vol. 80, no. 1, 2009.

[14] U. Banerjee, P. Bit, R. Ganguly, and S. Hardt, "Aggregation dynamics of particles in a microchannel due to an applied magnetic field," *Microfluidics and Nanofluidics*, vol. 13, no. 4, pp. 565–577, 2012.

[15] S. Kang and Y. K. Suh, "Direct simulation of flows with suspended paramagnetic particles using one-stage smoothed profile method," *Journal of Fluids and Structures*, vol. 27, no. 2, pp. 266–282, 2011.

[16] Q. Cao, Z. Wang, B. Zhang et al., "Targeting behavior of magnetic particles under gradient magnetic fields produced by two types of permanent magnets," *IEEE Transactions on Applied Superconductivity*, vol. 26, no. 4, Article ID 4401305, 2016.

[17] Q. A. Pankhurst, J. Connolly, S. K. Jones, and J. Dobson, "Applications of magnetic nanoparticles in biomedicine," *Journal of Physics D: Applied Physics*, vol. 36, no. 13, pp. R167–R181, 2003.

[18] G. De Las Cuevas, J. Faraudo, and J. Camacho, "Low-gradient magnetophoresis through field-induced reversible aggregation," *The Journal of Physical Chemistry C*, vol. 112, no. 4, pp. 945–950, 2008.

[19] C. Mikkelsen, M. Fougt Hansen, and H. Bruus, "Theoretical comparison of magnetic and hydrodynamic interactions between magnetically tagged particles in microfluidic systems," *Journal of Magnetism and Magnetic Materials*, vol. 293, no. 1, pp. 578–583, 2005.

[20] S. S. Leong, Z. Ahmad, and J. Lim, "Magnetophoresis of superparamagnetic nanoparticles at low field gradient: Hydrodynamic effect," *Soft Matter*, vol. 11, no. 35, pp. 6968–6980, 2015.

[21] Q. Cao, M. Liu, Z. Wang, X. Han, and L. Li, "Dynamic motion analysis of magnetic particles in microfluidic systems under an external gradient magnetic field," *Microfluidics and Nanofluidics*, vol. 21, no. 2, article no. 24, 2017.